Astro2020 Science White Paper

JWST/MIRI Surveys in GOODS-S

Thematic Areas: ☐ Planetary Systems ☐ Star and Planet Formation

☐Formation and Evolution of Compact Objects ☐ Cosmology and Fundamental Physics

☐Stars and Stellar Evolution ☐Resolved Stellar Populations and their Environments

☒Galaxy Evolution ☐Multi-Messenger Astronomy and Astrophysics

Principal Author:
Name: George Rieke
Institution: University of Arizona
Email: grieke@as.arizona.edu
Phone: 520-621-2832

Co-authors: (names and institutions)
Stacey Alberts, University of Arizona, USA
Irene Shivaei, University of Arizona, USA
Luis Colina, Consejo Superior de Investigaciones Cientificas, Spain
Hans Ulrik Nørgaard-Nielsen, Danmarks Tekniske Universitet, Denmark

Abstract (optional):

To illustrate some of the capabilities of the Mid-Infrared Instrument (MIRI) for JWST for studies of galaxy evolution, we discuss the Guaranteed Time Observer (GTO) programs 1207 and 1283, both centered in the GOODS-S field. These programs plan to: (1) measure the obscured star formation rates down to 10 $M_\odot$/yr and out to $z \sim 2.5$; (2) measure aromatic band strengths to constrain processes in galaxy interstellar media out to $z \sim 1.3$; (3) complete our inventory of active galactic nucleus types including very strongly obscured examples; (4) improve mass estimates for galaxies by providing a measurement at ~ 1 μm rest (for $z \geq 4$); and (5) help determine masses and ages of young stellar populations at $z > 8$.

Introduction: JWST/MIRI can provide answers to important open questions about galaxy evolution at $z \sim 1 - 3$, at the peak of star formation (SF) and active galactic nucleus (AGN) activity. First, MIRI can complete our picture of luminous star-forming galaxies. In this redshift range, a significant fraction of the star formation occurs in galaxies above 10^{11} $L_\odot$ and can be heavily obscured (Reddy et al. 2010, Wuyts et al. 2011, Madau & Dickinson 2014). SF rates (SFRs) from rest frame UV measurements become increasingly uncertain at high obscuration (Safarzadeh et al. 2017). A better alternative is to estimate the SFRs from the total infrared luminosity. However, of the available measurements, only the MIPS 24μm band approaches the necessary sensitivity (e.g., Elbaz et al. 2011), and it falls about a factor of five short of 10^{11} $L_\odot$ at z = 2. Multi-band MIRI surveys can easily reach 10^{11} $L_\odot$. Second, MIRI mid-IR photometry can also augment our inventory of AGNs. Although deep X-ray imaging is often relied upon for AGN samples, it is likely incomplete: (1) 36% of type-2 AGN are Compton thick and hence with suppressed X-ray outputs (e.g., Landbury et al. 2015); (2) 1/3 of infrared-bright quasars may be too absorbed to be detected in the X-ray (Del Moro et al. 2016); and (3) alternative identification methods suggest a very high incidence of AGN in massive galaxies, i.e. 37% for 0.3 < z < 1 (Juneau et al. 2011). Multi-band MIRI data will be able to identify heavily obscured AGN to complete our census.

MIRI can also contribute key insights to the Epoch of Reionization (EoR). Very deep MIRI images, incorporated with those of NIRCam, will help to characterize galaxies at z $\sim$ 4 and also at z > 8 (during the EoR).

Figure 1. Approximate layout of the JADES (NIRCam fields in gray), ultradeep 5.6μm MIRI (yellow), and MIRI multiband (magenta)surveys in the GOODS-S field. The ultradeep survey is centered on the HUDF. The actual layout of the surveys will depend on launch date and access to the field, and may also be adjusted slightly through further optimization.

Mid-IR Survey in GOODS-S: The US GTO GOODS-S program (#1207) will address these topics by: (1) imaging deeply at 21μm to reach galaxies of 10^{11} $L_\odot$ out to z = 2.5; (2) measuring aromatic feature strengths to probe the nature of the ISM in the same galaxies and also to refine the total infrared luminosity determinations; and (3) making a demanding search for heavily obscured AGN to complement the deep searches in the same field using X-rays, optical spectroscopy, and radio observations. The EC GTO observers (#1283) will obtain an extremely deep image at 5.6 μm to: (4) improve mass estimates for galaxies by providing a measurement at $\sim$ 1 μm rest (for z $\geq$ 4); and (5) study different phases of the EoR by determining masses and ages of young stellar populations at z > 8, exploiting the clean measurements of Balmer breaks it makes possible.

Program 1207 is for a MIRI multi-band survey. A variety of arguments suggest that 30 square arcmin (i.e., 15 MIRI fields) surveyed to the depth achieved in about one hour at 21μm will return 30 - 40 AGN of known types out to z $\sim$ 2.5 and detected at 10:1 signal to noise or higher, plus high quality measurements of some 2000 star forming galaxies. The EC team is planning a single ultra-deep exposure at 5.6μm within the area of the multi-band survey. An
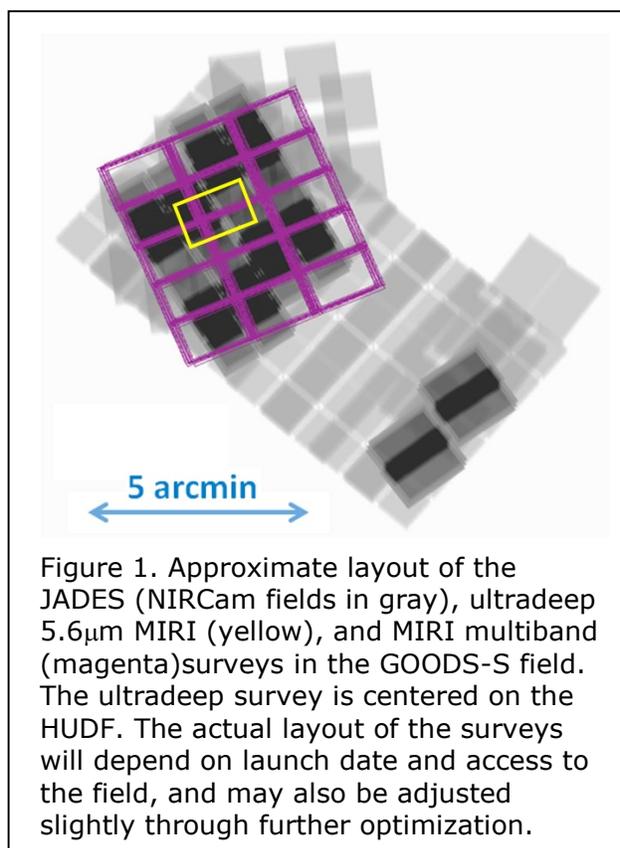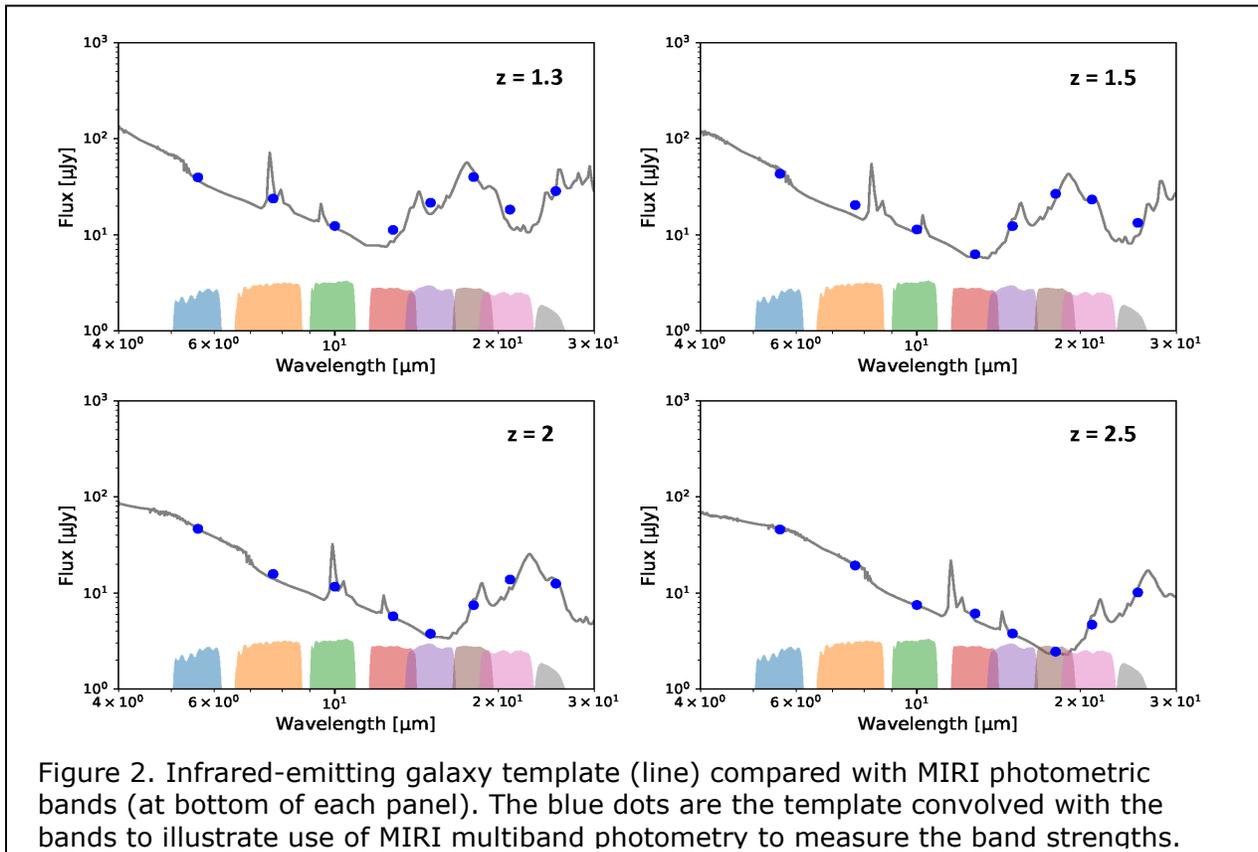
approximate layout for these surveys is shown in Figure 1. The science enabled by the MIRI surveys will benefit not only from the ultradeep NIRCam imaging (and accompanying follow up with NIRSpec), but from the uniquely deep imaging in this area with Chandra, XMM-Newton, HST, Spitzer, Herschel, ALMA, and the JVLA.

The multiband MIRI survey is focused on the peak of star formation and AGN activity at z of 1 to 3. The starting point for setting the integration times is that a SFR of 10 $M_\odot$/yr (total infrared luminosity of about 10^{11} $L_\odot$) at z = 2 will have a 21 μm flux density of ∼ 10 μJy (Kennicutt & Evans 2012, Shipley et al. 2016). This SFR falls below the Main Sequence for galaxies with mass > 10^{10} $M_\odot$; half an hour with MIRI will detect such a galaxy at $\geq$ 7 σ. The integration times for the shorter wavelength bands were set to obtain high SNR on AGN continua, with increased integration on some of the intermediate bands to characterize the aromatic bands. Shallower measurements are planned also at 25.5 μm to constrain the aromatic emission modeling for the brighter galaxies (and through stacking). This survey demonstrates the importance of the high angular resolution of JWST (0.75" PSF FWHM at 21μm). Spitzer measurements at 24μm (6" PSF FWHM) are confusion limited at about 50 μJy (Dole et al. 2004).

Obscured Star Formation at z = 2: The goal for star forming galaxies is to measure the obscured star formation down to the levels of activity below which it becomes relatively accurately determined from rest UV measurements alone, e.g., the IRX-β method (e.g., Salim & Boquien 2018). For luminous and relatively high metallicity galaxies, the 21μm

Figure 2. Infrared-emitting galaxy template (line) compared with MIRI photometric bands (at bottom of each panel). The blue dots are the template convolved with the bands to illustrate use of MIRI multiband photometry to measure the band strengths.

measurements (rest frame ∼ 7μm at z = 2) can return accurate measures of the obscured star formation directly, even though the measures must be based on the aromatic bands between 6 and 8μm rest wavelengths (e.g., Rujopakarn et al. 2013, Shipley et al. 2016). At lower luminosities the strength of these bands is diminished (Shivaei et al. 2017) so determination of SFRs will benefit by measuring their strengths directly using the multiple MIRI bands as illustrated in Figure 2 and comparing with star formation rates determined in other ways, e.g., Hα, Paβ and Paα for selected galaxies. The ability to determine accurate SFRs in this field will

be further enhanced by the ultradeep measurements with the JVLA at 3 and 6 GHz, by ALMA surveys, and by the ultradeep Herschel survey. The ~10" resolution imaging of the latter survey can be deconfused using higher resolution data in the other bands. This program should yield the most accurate estimates of galaxy total infrared luminosities at z ~2 possible until a large space-borne far infrared telescope becomes available.

As shown in Figure 2, the photometry will determine relative strengths of the aromatic bands at 3.3, 7.7, and 11.3µm out to z ~ 1.3 (see also Inami et al. (2018)), revealing the state of the aromatic molecules. From Allamandola et al. (1999), the 3.3µm feature is produced almost exclusively by ionized aromatic molecules, which are also bright in the 11 - 14µm complex, whereas the 7.7µm complex is emitted by ionized aromatic molecules. Understanding the state of the aromatics will illuminate the microscopic processes that regulate carbon nucleation and molecular growth in the interstellar medium. As examples: (1) the ratio of the 11.3 and 7.7µm feature strengths depends on the ionization state of the ISM (e.g., Galliano et al. 2008); and (2) the 7.7µm complex is suppressed in the vicinity of AGN (Diamond-Stanic & Rieke 2010).

Search for Obscured AGNs: A second goal for the multiband survey is to identify AGNs. Mid-infrared color selection with the MIRI filters can take advantage of the minimum in star forming galaxy spectral energy distributions at $4 - 5$µm, on the Rayleigh Jeans tail of the stellar photospheric emission, but short of the wavelengths dominated by the aromatic bands. Figure 2 shows how the MIRI bands can isolate this minimum and search for obscured AGN whose emission would fill it in. A more general technique is to use diagnostic diagrams that isolate the
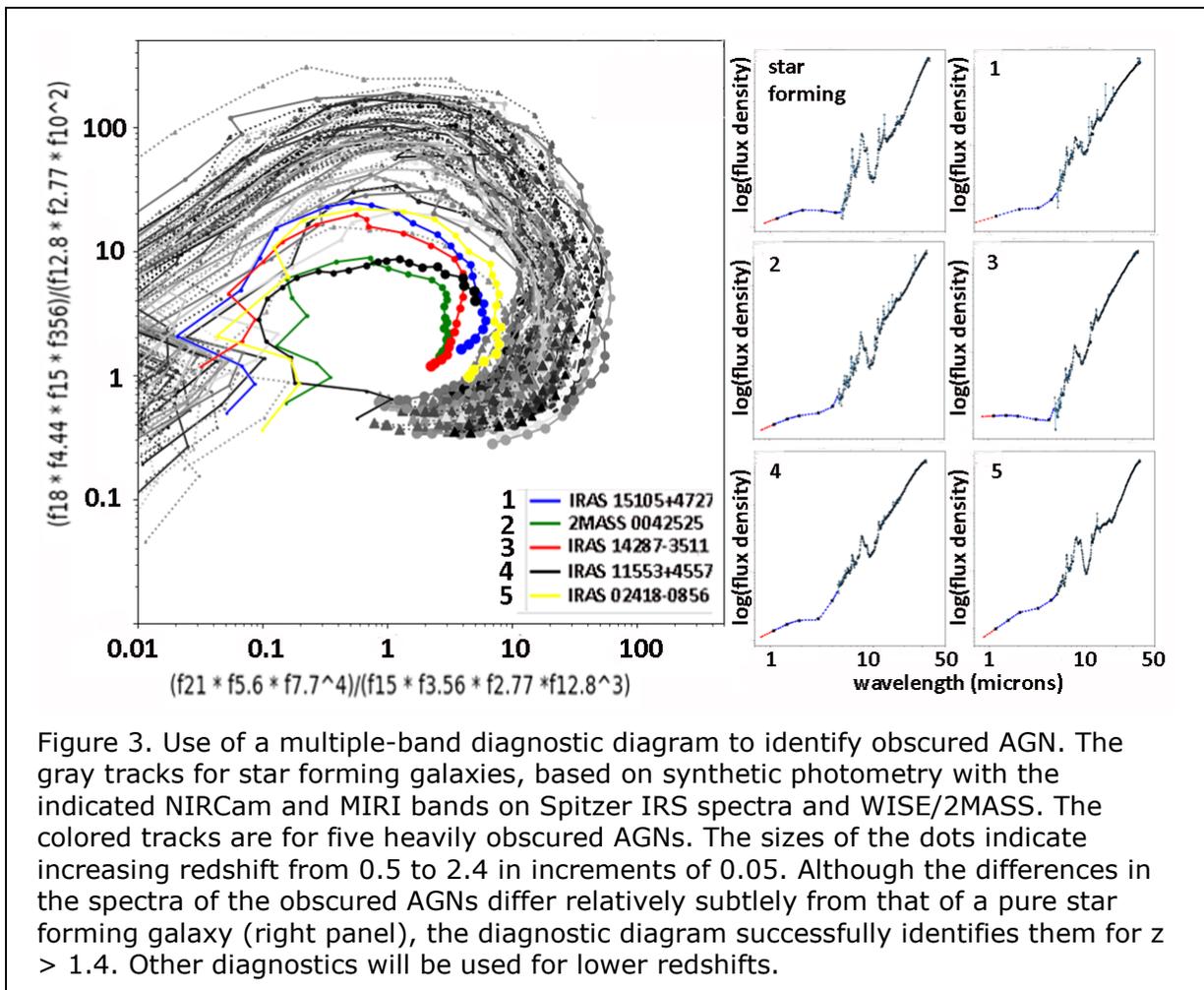

Figure 3. Use of a multiple-band diagnostic diagram to identify obscured AGN. The gray tracks for star forming galaxies, based on synthetic photometry with the indicated NIRCam and MIRI bands on Spitzer IRS spectra and WISE/2MASS. The colored tracks are for five heavily obscured AGNs. The sizes of the dots indicate increasing redshift from 0.5 to 2.4 in increments of 0.05. Although the differences in the spectra of the obscured AGNs differ relatively subtly from that of a pure star forming galaxy (right panel), the diagnostic diagram successfully identifies them for z > 1.4. Other diagnostics will be used for lower redshifts.

minimum using many of the colors measured with JWST, in analogy with the methods using Spitzer IRAC bands or WISE ones. Such diagrams can be much more powerful than previous ones given the many additional bands available with JWST, as shown in Figure 3.

NIRCam plus MIRI imaging will allow us to decompose the optical to MIR SEDs of galaxies into host and AGN components, linking AGN properties such as bolometric luminosity to host galaxy properties such as morphology, SFR, etc. An important application of the multiple ways to identify AGN in the HUDF is to cross-calibrate the methods and reduce the uncertainties in the quasar luminosity function (QLF). The behavior of the QLF vs. redshift is fundamental to our understanding of how supermassive black holes grow, yet there is wide disagreement on its form at low luminosities (e.g., Masters et al. 2012, McGreer et al. 2013, Giallongo et al. 2015). Current identifications in the X-ray are up to 30 times deeper (in terms of AGN luminosity) than optical and infrared surveys (Hopkins et al. 2007). The MIRI images will match the deep X-ray identifications and will allow cross-calibration to the faintest limits known.

The MIRI spectral range suffices to determine AGN infrared luminosities accurately (Lyu & Rieke 2017, Lani et al. 2017). Therefore, the combination of X-ray, UV, optical, and infrared measurements of AGN in this field will determine accurate *total* luminosities and new insights to the black hole accretion rates (BHARs). The BHARs compared with the SFRs provide critical insight to the co-evolution of star formation and black hole growth. Our determination of BHARs for a complete sample of AGNs, including any heavily obscured examples, will become the foundation for correcting studies of larger samples with less complete AGN identification to obtain accurate average integrated BHARs.

NIRSpec Followup: To confirm the conclusions reached from the MIRI color modeling, we will select a sample of sources for NIRSpec Micro-Shutter Array spectroscopy at resolution R = 1000. Three NIRSpec pointings will cover of our survey field, and we have set the integration time to reach signal to noise of about 3 at Hα of 1×10^{-18} erg/s/cm^2, i.e., star formation rates of about 1 M$_\odot$/yr at z ~ 2. We will use all three NIRSpec bands to get full coverage from 1 - 5.2 μm with emphasis on the 1 - 3 μm range to measure the rest frame optical region.

The NIRSpec spectra enable a number of investigations. For the star forming galaxies, we will reconcile use of hydrogen recombination lines, mid-infrared and far-infrared excess, UV excess, radio luminosity, and X-ray emission as measures of star formation rates. This work will be critical to interpretation of our own survey and also for other JWST surveys that will not have such a rich ancillary data set to compare methods. Our spectra will also allow determining oxygen abundances, and, combining with the modeling of the multi-band MIRI photometry and SFRs measured through the multiple available techniques, we will be able to probe the behavior of the aromatic bands with redshift and metallicity. The availability of Hβ and [OIII] will identify AGNs that do not dominate the mid-IR and to test AGN identification methods.

Ultradeep Survey in the HUDF: The parameters for the ultradeep 5.6μm survey (program 1283) are based on the study by Bisigello et al. (2017). The measurements should reach a detection limit of 17 nJy or 28.3 AB, S/N = 4.0. This survey will provide rest-frame photometry near 1μm for hundreds of z ~ 4 galaxies; by providing better access to the emission of red giant stars, these observations will improve the constraints on the ages of the stellar populations. The MIRI observations become even more helpful in deriving properties of galaxies with nebular continuum and line emission (because of the lack of strong lines at the MIRI rest wavelengths). The program will also detect a few tens of z > 7.5 EoR sources. The MIRI and NIRCam observations together will constrain the stellar masses and specific star formation rates of galaxies at z > 8 significantly more tightly than with NIRCam data alone. Finally, the NIRCam and MIRI imaging goes far deeper and at higher angular resolution than any previous surveys at wavelengths longer than 3μm. Very long integrations with IRAC are limited by confusion noise given the 1.2 arcsec pixels, whereas the much smaller MIRI beam, 0.2" FWHM at 5.6μm, virtually eliminates confusion as well as locating the emission with an accuracy commensurate with that for HST, JVLA, ALMA and the MUSE ground layer AO system. The depth and ability to pinpoint the location of the sources make it plausible that new types of sources will be revealed. In such cases, the extended wavelength coverage provided by MIRI and NIRCam together could be critical to determining their natures.

References

Allamandola, L. J., Hudgins, D. M., & Sandford, S. A. 1999, ApJL, 511, 115

Bisigello, L., Caputi, K. I., Colina, L. et al. 2017.ApJS, 231, 3

Del Moro, A., Alexander, C. M., Bauer, F. et al. 2016, MNRAS, 456, 2105

Diamond-Stanic, A. M., & Rieke, G. H. 2010, ApJ, 724, 140

Dole, H., Rieke, G. H., Lagache, G. et al. 2004, ApJS, 154, 93

Elbaz, D., Dickinson, M., Hwang, H. S. et al. 2011, A&A, 533, A19

Galliano, F., Madden, S. C., Tielens, A. G. G. M., Peeters, E., & Jones, A. P. 2008, ApJ, 679, 310

Giallongo, E., Grazian, A., Fiore, F. et al. 2015, A&A, 578A, 83

Hopkins, P. F., Richards, G. T., & Hernquist, L. 2007, ApJ, 654, 731

Inami, H. Armus, L., Matsuhara, H. et al. 2018, A&A, 617, A130

Juneau, S., Dickinson, M., Alexander, D. M. et al. 2011, ApJ, 736, 104

Kennicutt R. C. & Evans N. J., 2012, ARA&A, 50, 531

Landbury, G. B., Gandhi, P., Alexander, D. et al. 2015, ApJ,809, 115

Lani, C., Netzer, H., & Lutz, D. 2017, MNRAS, 471, 59

Lyu, Jianwei, & Rieke, G. H. 2017, ApJ, 841, 76

Madau, P., & Dickinson, M. 2014, ARAA, 52, 415

Masters, E., Capak, P., Salvato, M. et al. 2012, ApJ, 755, 169

McGreer, I. D., Jiang, L., Fan, X. et al. 2013, ApJ, 768, 105

Reddy, N. A., Erb, D. K., Pettini, M. et al. 2010 ApJ, 712, 1070

Rujopakarn W., Rieke G. H., Weiner B. J., et al. 2013, ApJ, 767, 73

Salim, S., & Boquien, M. 2018, arXiv 181205606

Safarzadeh, M., Hayward, C. C., & Ferguson, H. C. 2017, ApJ, 840, 15

Shipley, H. V., Papovich, C., Rieke, G. H., Brown, M J. I., & Moustakas, J. 2016, ApJ, 818, 50

Shivaei I., Reddy, N. A., Shapley, A. E. et al. 2017, ApJ, 837, 157

Wuyts, S., Forster Schreiber, N. M., Lutz, D. et al. 2011, ApJ, 738, 106